NOAA Technical Memorandum EDS CEDDA-2

CHARACTERISTICS OF THE LOWER ATMOSPHERE NEAR SAIPAN, APRIL 29 TO MAY 16, 1945

Joshua Z. Holland

Washington, D.C.
April 1975

noaa NATIONAL OCEANIC AND ATMOSPHERIC ADMINISTRATION / Environmental Data Service

NOAA TECHNICAL MEMORANDA

Environmental Data Service, CEDDA Series

r for Experiment Design and Data Analysis (CEDDA) became part of NOAA's Environmental Data Service in 1972 and was given the responsibility for data management and activities related to major international scientific field experiments.

Formerly the Barbados Oceanographic and Meteorological Analysis Project (BOMAP), CEDDA is still concerned with analyses of data collected during the Barbados Oceanographic and Meteorological Experiment (BOMEX), conducted in 1969, and will continue to issue publications pertaining to BOMEX as part of the EDS BOMAP series.

NOAA Technical Memoranda in the Environmental Data Service CEDDA series will serve to disseminate information related to the 1974 Global Atmospheric Research Programme (GARP) Atlantic Tropical Experiment (GATE), as well as other forthcoming international field investigations.

Memoranda in the EDS CEDDA series are available from the National Technical Information Service, U.S. Department of Commerce, Sills Bldg., 5285 Port Royal Road, Springfield, Va. 22151. Price: Paper cover prices vary; $2.25 for microfiche. Order by accession number shown in parentheses at end of each entry.

EDS CEDDA-1 Omega Wind-Finding Capabilities: Wallops Island Experiments. Donald T. Acheson, October 1973, 77 pp. (COM-74-10039)

NOAA Technical Memorandum EDS CEDDA-2

CHARACTERISTICS OF THE LOWER ATMOSPHERE NEAR SAIPAN, APRIL 29 TO MAY 16, 1945

Joshua Z. Holland

Washington, D.C.
April 1975

UNITED STATES
DEPARTMENT OF COMMERCE
Frederick B. Dent, Secretary

NATIONAL OCEANIC AND
ATMOSPHERIC ADMINISTRATION
Robert M. White, Administrator

Environmental Data
Service
Thomas S. Austin, Director

PREFACE

The report presented herein was transmitted to the Headquarters, U.S. Army Air Forces Weather Service, Pacific Ocean Area, on June 11, 1945. It was prepared by me, based on a field program carried out with the assistance of Lt. Earl Sargent of the U.S. Army Air Force. It is the meteorological part of an investigation under the direction of D. E. Kerr of the MIT Radiation Laboratory. The overall investigation had to do with factors affecting the performance of a radar on Saipan. The report was originally classified "Confidential." I have been encouraged to publish the meteorological part, even at this late date, because of the recent increase of interest in the atmospheric boundary layer over the tropical ocean and because data of this kind that are available are still largely limited to the Atlantic and Caribbean areas. It is interesting to see that the structure found over the western Pacific Ocean is identical to that found over the western Atlantic, despite considerable differences in observational technique.

I had considered reworking this material to condense it and to overcome some slight quaintness of notation and terminology. However, I have become convinced that it will be quite satisfactory from the standpoint of readability, and highly desirable from the standpoint of avoiding further delays in its "seeing the light of day," to present the report exactly in its original form except for addition of a few explanatory footnotes and the elimination of two final sections containing suggested extensions and recommendations that were not an essential part of the research and are no longer of interest.

Joshua Z. Holland
August 1973

CONTENTS

CHARACTERISTICS OF THE LOWER ATMOSPHERE NEAR SAIPAN, APRIL 29 TO MAY 16, 1945

Joshua Z. Holland
Center for Experiment Design and Data Analysis
National Oceanic and Atmospheric Administration
Washington, D.C. 20235

Abstract. This is the meteorological part of a World War II investigation of the performance of a U.S. Army search radar located on Saipan in the Marianas Islands. Thirty detailed temperature and humidity soundings of the lowest 10,000 ft over the ocean were made with a mercurial psychrometer aboard a PBY flying boat. The data are analyzed to show typical characteristics of the vertical structure. The existence of a layer of strong gradient of M (the modified index of refraction) between the lowest level sampled (20 to 30 ft) and the surface is inferred. A layer of nearly constant potential temperature and mixing ratio is generally found extending up to an altitude that averages 1,700 ft and ranges from 1,000 to 2,600 ft. This moist "stirred layer" is generally topped by a stable transition layer. Above this a drier layer with a temperature lapse rate between dry and moist adiabatic, containing cumulus clouds, extends up to a second stable layer, the "trade inversion." Seven of the 12 aircraft soundings that reached 8,000 ft, and 16 out of 21 radiosonde observations taken at Saipan during this period, showed such a stable layer with an average base altitude of 5,000 ft.

1. GENERAL

1.1 Objectives

The objectives of the present study are as follows:

(1) To make detailed low-level meteorological soundings in the vicinity of Saipan; to analyze these soundings in terms of the distribution of the "modified index of refraction," and to determine the effect of meteorological factors on the coverage of the AN/CPS-1 radar on Mt. Tapotchau, Saipan.

(2) To suggest (a) significant meteorological factors to be looked for in similar studies in other locations, such as Iwo Jima and Okinawa; (b) requirements for such investigations; and (c) suitable methods for conducting such investigations.

1.2 Description of Investigation

The 30 airplane soundings discussed here were made during the period April 29 to May 16, 1945. The instrument used for measuring temperature and humidity was a mercurial psychrometer, constructed at the MIT Radiation Laboratory, and installed on the top of the nose of a PBY flying boat, well forward of the engines. A radiation shield was constructed out of two fruit cans with the flat ends removed, joined end to end. The thermometer bulbs were protected by the shield from direct illumination by the sun, but it is possible that the readings were influenced somewhat by reflected radiation from the inner surface of the shield. No correction was made for this effect. Two observers were required for the soundings. One observer read the psychrometer, while the other read the pressure altimeter and airspeed indicator and recorded all data.[1] Temperatures were read to the nearest 0.1°C. After several unsuccessful attempts at determining the dynamic temperature correction by flying at different airspeeds at a constant altitude and plotting temperature readings as a function of airspeed, the correction $0.8(v/100)^2$ (which appeared to be a reasonable value and where v = airspeed, probably in knots) was added to both temperature and wet-bulb temperature readings. Soundings were made to the northeast and east of Saipan (where air traffic was very light) at varying distances from the island. Most soundings were within 100 mi of Saipan, but on May 9 soundings were made 50, 100, and 150 mi east of Saipan, in order to study the horizontal variations of the M-distribution[2] over the entire radar range. All the soundings have been included in the averages, because they are considered to be equally representative of the climate. No sea-surface temperatures were measured directly, but were extrapolated from the dry-adiabatic lapse rate in the stirred layer. No significant variation in these sea-surface temperatures was noted. Soundings were made around midday and early afternoon, and mostly in relatively good weather. Only on May 4 and 14 were flights made in showery weather. Of the 30 soundings, 25 reached 4,000 ft and 12 exceeded 8,000 ft.

The other data used to complete the picture include the Saipan radiosonde, winds-aloft (rawinsonde) and surface observations. The radiosonde data were obtained from the original records at Kagman Point Upper Air Section, Saipan, where more levels are recorded than are transmitted in the final message, and temperatures are recorded to the nearest 0.1°C. Although the radiosonde record is unsuitable for detailed analysis of the lower 2,000 ft, it agrees well with the psychrometer observations in the middle layer (approximately 2,000 to 4,000 ft), particularly in moisture content. The complete set of observations makes a self-consistent picture, possibly not quantitatively representative of the entire season, but probably a reasonably good sample.

---

[1] The soundings were of the "stepped" type. Each reading was taken on a straight and level leg of a 1- or 2-min duration--long enough to allow the psychrometer to approach equilibrium.

[2] The definition of M is given in the following section.

2. SUMMARY OF ATMOSPHERIC CHARACTERISTICS

2.1 Description of Model of the Lower Atmosphere

From an examination of the airplane and radiosonde soundings, it became apparent that the structure of the lower atmosphere is characterized by the following features:

(1) There is a lower stirred layer in which the potential temperature and mixing ratio are uniformly distributed with height and in which the water vapor is unsaturated at the surface. The potential temperature and mixing ratio are nearly constant from day to day.

(2) At the top of the stirred layer there is a stable transition zone, frequently showing a small temperature inversion. In this zone the mixing ratio drops off more or less abruptly with height. The mixing-ratio lapse rate is greatest in the clear spaces between clouds, and least within the cumulus clouds. The temperature inversion, likewise, is most marked in the clear spaces between clouds, and absent within the air columns containing the clouds.

(3) Above this transition zone there is a layer of intermediate moisture content which shows a slow decrease with height, and varies appreciably between cloud and clear spaces. The temperature lapse rate in this layer is usually between the moist and dry adiabatic, but is sometimes less than the moist adiabatic.

(4) At the top of this intermediate layer, there is usually a second stable layer, in which the mixing ratio shows a more rapid decrease with height. The air above this second transition layer is dry upper air. Frequently this inversion disappears (or is displaced to a much higher level), and then the intermediate mixing ratios extend to abnormally great heights. This second inversion is the upper limit of general low cloud development, but may be penetrated by individual towering cumuli.

2.2 Characteristic Quantities

Selected characteristic quantities for each sounding, together with maximum, minimum, and average observed values of each characteristic quantity, are contained in table 1 (airplane soundings) and table 2 (radiosondes). The average values are used in the construction of figure 1.

The following data are obtained from an analysis of the airplane observations. The Saipan radiosonde was too much influenced by surface heating, cooling, and frictional stirring, and lacking in sufficient detail for use in evaluating most of these features.

(1) θ_{st}: The potential temperature of the stirred layer. This was obtained by drawing the best dry-adiabat through the plotted temperatures in the stirred layer, and assuming a surface pressure of 1,013 mb.

(2) T_s: The temperature of the intersection of the θ_{st} line with the 1,013-mb isobar. Assuming neutral thermal equilibrium, this is equal to the sea-surface temperature. This assumption appears justified in view of the following considerations:

(a) The known horizontal homogeneity of the sea-surface temperature in this region, and the long trajectory of the air over a uniform water surface.

(b) The absence of any observed stable or superadiabatic temperature lapse rates near the sea surface during the course of these flights.

(c) The near-constancy of θ_{st} from day to day under various weather conditions.

(3) w_s: The saturation mixing ratio corresponding to T_s at 1,013 mb. This is the mixing ratio in the air immediately adjacent to the sea surface.

(4) $\overline{w}_{st}$: The average value of the mixing ratio in the stirred layer. Although w was nearly constant in each sounding, it varied more from one sounding to another than did θ_{st}. In some cases a scattering of values of w about the mean was obtained in the stirred layer.

(5) ΔM_s: The deficit of modified index of refraction[3] in the bottom of the stirred layer. This is equal to $M_s - M_{st} = 79/T_s 2 \times 4{,}800\ (e_s - e_{st})$, where e_{st} is the vapor pressure in the stirred layer measured at 1,013 mb atmospheric pressure.

(6) H_1: The height of the top of the stirred layer. At this point θ and w change abruptly with increasing height.

(7) H_{c1}: The measured height of the base of the low clouds. These heights were determined visually by the observer in the airplane at the moment of passage through the cloud level.

(8) Δw_1: The decrease of mixing ratio through the transition layer at the top of the stirred layer. This is the difference between $\overline{w}_{st}$ and the value of w at the top of the narrow layer of rapid moisture decrease.

(9) ΔT_1: The change in temperature through the transition layer determined by Δw_1.

(10) Δh_1: The depth of the transition layer determined by Δw_1.

(11) ΔM_1: The change in modified index of refraction through the transition layer.

---

[3]Modified index of refraction $M = 79(P + 4{,}800e/T)/T + 0.0478h$, where T = temperature in degrees centigrade, P = pressure in millibars, e = vapor pressure in millibars, and h = height in feet.

(12) v_{20}: The windspeed at 2,000 ft, obtained from the Saipan rawinsondes.

(13) ΔT_{20-40}: The change in temperature from 2,000 to 4,000 ft. At the dry-adiabatic lapse rate, $\Delta T_{20-40} = -6.1^{\circ}C$. At the saturated-adiabatic lapse rate, $\Delta T_{20-40} = -2.6^{\circ}C$.

(14) $\bar{w}_{25-40}$: The average mixing ratio in the layer from 2,500 to 4,000 ft. This is a measure of the moisture content of the intermediate layer. The lower limit was chosen so as always to be above the transition layer.

(15) Weather (general): The prevailing weather conditions as observed from the airplane.

(16) Weather (sounding): Actual weather phenomena encountered by the airplane during the sounding.

The following data are tabulated in table 2 for the Saipan radiosondes during the period from May 6, 1300 GMT, to May 16, 1300 GMT. The original records were used. Approximate values of H_2 and Δh_2 were obtained from plotted radiosonde soundings in AAF Weather Central, Guam, for the period April 28, 1300 GMT, to May 6, 0100 GMT, and are shown in the time cross section (fig. 2, facing page 20), but are not included in the averages.

(1) ΔT_{20-40}.

(2) $\bar{w}_{25-40}$.

(3) H_2: The height of the base of the second stable layer. This zone appeared in 15 of the 21 radiosonde soundings. The approximate values obtained for the preceding week exceeded 6,000 ft in five cases. The average value obtained during the period covered by accurate radiosonde data may be abnormally low.

(4) Δw_2: The change in mixing ratio through the second stable layer.

(5) ΔT_2: The change in temperature through the second stable layer.

(6) Δh_2: The depth of the second stable layer.

(7) dT/dh_{100}: The lapse rate in the layer just below 10,000 ft. The temperature at 10,000 ft and the temperature at the next point, at least 100 m lower, were used. The dry-adiabatic lapse rate is $3.0^{\circ}C$/1,000 ft, and the moist adiabatic is $1.5^{\circ}C$/1,000 ft.

(8) T_{100}: Temperature at 10,000 ft.

(9) w_{100}: Mixing ratio at 10,000 ft.

The following data are plotted in time sequence in figure 2 (facing p. 20):

(1) Three-hourly Saipan surface observations, plotted according to the station model used in synoptic analysis.

(2) Winds at 2,000 and 4,000 ft, from the Saipan rawinsonde observations.

(3) H_1 from airplane observations.

(4) H_2 from Saipan radiosondes.

(5) H_{c1} from airplane and surface measurements.

(6) Cloud and weather cross section based on airplane and surface observations.

3. FRICTIONAL BOUNDARY LAYER

3.1 Theory

According to R. B. Montgomery (1944) under conditions of neutral thermal equilibrium between the frictionally stirred lower air and the sea surface, the water vapor at the base of the homogeneous stirred layer must be unsaturated. There is, then, a moisture deficit at the base of the stirred layer with respect to the saturated air immediately adjacent to the ocean surface. The shallow transition layer between the surface and the base of the homogeneous layer is known as the "frictional boundary layer." This layer has been shown by theory and observation to occupy roughly one-tenth of the "layer of frictional influence" that extends to the top of the stirred layer. The rapid transfer of water vapor upward through the boundary layer is compensated for by the loss of moisture to the relatively dry air above the stirred layer, both by mechanical stirring and by thermal convection. (In some cases of large vertical vapor-pressure gradients at the top of the stirred layer, molecular diffusion may play an appreciable role.) This dynamic equilibrium maintains a nearly constant mixing ratio in the stirred layer.

Within the frictional boundary layer, the windspeed, potential temperature, and mixing ratio vary logarithmically with height, according to the equation:

$$\frac{dq}{d\ln(h)} = \Gamma(q_s - q_b) ,$$

where q_b is a representative value of the quantity q at a height b, and q_s is the value of q at the sea surface. Since in the case of neutral equilibrium $\theta_s = \theta_b$, $d\theta/d\ln(h) = 0$ in the boundary layer as well as in the remainder of the friction layer. Montgomery (1944) used $\Gamma = 0.08$ for b = 50 ft to calculate the vertical distribution of the modified index of refraction, M, in the boundary layer. At first M decreases rapidly, then more slowly, until

$dM/dh = 0$ at the height $d = 2$ ft $\times \Delta M$, where ΔM is equal to M at the surface minus M in the stirred layer extrapolated linearly to the surface. The height d is known as the "duct height." When the sea-surface temperature and pressure are constant, ΔM is a function of Δw alone. Table 3 gives e_s, w_s for varying values of T_s. Table 4 gives ΔM as a function of Δw at $T_s = 28°C$. Mongomery's relation between d and ΔM is admittedly over-simple and based on insufficient data (particularly for our purpose, since all his observations were made over middle-latitude coastal waters). Nevertheless, he ventures the estimate that the large vertical gradients of w and M will be confined to the lower 100 ft. With data obtained from the U.S. Weather Bureau Atlas of Climatic Charts of the Oceans (1938) he predicts that a permanent M-inversion extending to roughly 30 ft will be found in the Guam area. Both these statements are borne out by our measurements, although the average values of ΔM as given by the climatic charts are less than half the observed values (his charts showing $\Delta M = 19$ for March, April, and May and $\Delta M = 21$ for June, July, and August).

The assumption of neutral thermal equilibrium is supported by the climatic charts, which show a temperature deficit of about 0.3°C for this region at 1300 GMT in March, April, and May. This is equal to the diurnal variation of the sea-surface temperature in the tropics, according to Sverdrup (1942), and probably somewhat less than the diurnal variation of the surface air temperature (Petterssen, 1940). Furthermore, Montgomery (1944) finds that the entire homogeneous layer will adjust to horizontal surface-temperature gradients of a degree or two in a few miles. It is very unlikely that stronger gradients exist in the open ocean in the vicinity of Saipan. All but one of 28 surface temperatures obtained by dry-adiabatic extrapolation from airplane observations in the stirred layer were within 0.3°C of the average value of 27.7°C, which agrees closely with the mean sea-surface temperature for this season. (The CINCPAC-CINCPOA Bulletin No. 4-45 gives, for the 5° square including Saipan, 81°F for April and 82°F for May; our average for April 28 to May 16 is 81.9°F.)

3.2 Measurements

Although 14 of the 30 soundings discussed here include measurements below 30 ft, no definite large vertical gradient of potential temperature or mixing ratio appears at the base of any of the soundings. However, assuming neutral thermal equilibrium, large M-deficits were always found, the average value of ΔM being 44 units. If $d = 2$ ft $\times \Delta M$, the M-inversion should have begun to appear at about 90 ft, with strong vertical gradients of w and M between 50 and 20 ft. It is evident that the approximation $d = 2$ ft $\times \Delta M$ is not applicable in this area. Γ is dependent on wind velocity and stability, and the value 0.08 may be based on incorrect values for this climate. Nevertheless, it seems safe to conclude from our measurements that a very low, intense duct is always present. Montgomery's predicted duct height of 30 ft seems not unreasonable, but detailed measurements will be necessary before anything definite can be said about its structure.

3.3 Relation of ΔM_s to Other Characteristic Quantities

In spite of the lack of direct measurements of duct height, some idea of the probable variation of intensity of the surface duct can be obtained from the variation of ΔM_s. The small variation of ΔM may be related to some of the other characteristics of the lower atmosphere.

Since T_s is so nearly constant, it may be expected that ΔM_s will be mainly dependent upon Δw_s, which in turn depends upon $\overline{w}_{st}$. Figure 3 shows the observed values of ΔM_s plotted against the corresponding values of w_{st}. It is seen that the points generally fall within three M-units of the line $\Delta M_s = 7(23.1 - \overline{w}_{st})$. The value of 23.1 in this empirical equation is the surface value of w, which agrees well with the average observed value of 23.0. Thus, in the vicinity of Saipan, in this season, it is only necessary to know the value of w in the stirred layer in order to make an accurate estimate of the M-deficit.

The mixing ratio in the stirred layer ($\overline{w}_{st}$) is related to the height of the turbulence inversion (H_1). It is seen from figure 4 that the higher the mixing ratio, the lower is the inversion. The inversion usually occurs just below the condensation level, which varies with the mixing ratio, as described in section 4. We can conclude that the surface duct will be strongest when the cloud level and the turbulence inversion are highest.

The extent to which the stirred layer is distorted by local effects may be judged from the sounding on May 8, 1520 GMT. On this occasion, readings between 500 and 1,500 ft were taken over Saipan harbor, in the lee of the island. In this layer, the mixing ratio was 15.2, as compared with values greater than 16 in the lowest 500 ft and in other soundings made on the same day east of the island. This dry air had probably subsided from above the stirred layer after passing across the 1,500-ft ridge in the center of the island.

4. TURBULENCE INVERSION

4.1 Theory

In a completely stirred layer the air mass is vertically homogeneous; that is, the mixing ratio and potential temperature are constant up to the condensation level, and change at the saturated rate above that level. If the stirred layer extended above the condensation level, an overcast would be present at that level. But since scattered cumulus clouds are usually observed rather than a low overcast, it may be inferred that the stirred layer does not reach the condensation level except in patches. Between the clouds there must be a stable layer that sets an upper limit for vertical stirring immediately below the condensation level. Furthermore, just as the frictional stirring results in a moisture deficit at the base of the homogeneous layer, it should also result in a moisture excess at the top of that layer, when compared with the unstirred (and probably descending) air between the cumulus clouds. This inversion will be absent in the air columns containing clouds. Between clouds, however, it may be strong enough to show a decrease of modified index with height.

Theoretically (Byers, 1944), the height of the layer of frictional influence, H, is proportional to the windspeed, and increases with increasing surface roughness and decreasing stability, temperature, and latitude. The roughness is expressed by a length Z, the roughness coefficient, which is believed to be about 1/30 the height of the roughness elements. The values of H in table 5 were obtained from Byers (1944), using latitude 15°. The temperature and stability values used in the construction of this table were not known, but were probably representative of middle-latitude conditions.

4.2 Measurements

A stable layer was found at the top of the homogeneous layer in every airplane sounding except those taken through clouds. The height (H_1) and strength (Δw_1, ΔT_1, Δh_1, ΔM_1) for each sounding and the average for the series are given in table 1. The average structure of the H_1 inversion is shown in figure 1. It is seen that the average height of the top of the stirred layer is 1,700 ft, which is 50 ft less than the average cloud height observed. Based at this height there is a stable layer whose average depth is 240 ft, in which the temperature drops only 0.1°C. The transition from the moist stirred layer to the relatively dry air above takes place mainly in this narrow layer, the mixing ratio showing an average drop of 2.0 g/kg from its average value of 16.8 in the stirred layer. In most cases a weak duct was present; the average decrease was 4 M-units. The strongest duct in this zone was observed on May 9, with a decrease of 20 M-units in 100 ft. This persistent duct, which ranged in height from 1,000 to 2,600 ft, might be expected to cause occasional super-refraction of radiation from a radar set located at 1,500 ft, particularly when the inversion is slightly lower and more intense than average.

In two cases (April 29, 1046 l.t., and May 12, 1445 l.t.) an inversion was found at the top of a layer of flat cumulus clouds. With these exceptions, all the observed M-inversions occurred in the clear spaces between clouds. In several cases, also, two inversions were found in the vicinity of the cloud base. Since both inversions frequently showed weak ducts, they were both included in the averages. It is possible that these soundings represent a transitional condition, and that each of the two inversions is the predominating one over a different area or period of time.

The measurements of the depth of the transition layer (Δh_1) cannot be regarded as sufficiently accurate for refined gradient calculations, since of 31 values measured, 17 were between consecutive points in the sounding. The lower 55 percent of the Δh_1 values, then, were determined by the spacing between readings, and might have been considerably smaller had more detailed measurements been made.

No clear indication of the height or strength of the H_1 inversion was found in the Saipan radiosonde soundings. Surface heating and cooling, as well as increased frictional stirring due to passage over land, cause great changes in the lower 2,000 ft. In any case, the radiosonde is not suitable for direct measurement of such fine vertical variations.

4.3 Related Atmospheric Characteristics

Wind Velocity. Windspeeds at 2,000 ft, as measured by the Saipan rawinsondes, varied from 2 to 19 mi/h at the times of the airplane soundings. The corresponding winds at 4,000 ft varied from 2 to 24 mi/h. No positive correlation appears to exist between windspeed and height of the H_1 inversion. From table 5 it would be expected that H_1 would vary from about 1,000 to 8,000 ft, but H_1 is lower and much more steady than this. However, the strongest winds were observed under conditions of strong convective activity (fig. 2), and probably do not represent the mean wind flow. The H_1 inversion was found to be lowest under these same weather conditions, as discussed more fully below. Since both strong winds and instability would be expected from the turbulence theory to raise rather than lower the inversion level, it may be concluded that this level is determined more by the strength of local subsidence associated with individual convective cells than by prevailing stability and windspeed.

Cloud Level. It was indicated in section 4.1 above that the prevalence of scattered cumulus clouds rather than a low overcast suggested the presence of an inversion just below the condensation level. It was also noted in section 3.3 that the higher the mixing ratio, the lower is the turbulence inversion. The adiabatic condensation level, then, and with it the cloud level, should lower with a decrease in H_1. This is shown in figure 5. It is seen that although H_1 and H_{c1} have the same mean value (1,800 ft), H_1 has a greater range of variation than H_{c1}. From figure 4 we also see that the lowest inversions occur at about 85 to 90 percent relative humidity, while the highest are at about 100 percent. The cloud height generally occurs at about the 95 percent relative humidity level. Thus the moisture content of the stirred layer does not vary enough with height of the inversion to keep the top of the stirred layer at 95 to 100 percent relative humidity. Instead, the highest inversion occurs at the top of a layer of scattered, flat cumuli, while the lowest occurs in the large, perfectly clear (of low clouds) areas between large, isolated cumulonimbi, and below the general cloud bases. The relation works both ways; under showery conditions moisture is added to the stirred layer by falling rain as well as by evaporation from the sea surface. This lowers the cloud level, but at the same time the descending dry currents must reach lower in order to compensate for the larger ascending moist currents, lowering the H_1 inversion between clouds. For example, on May 14, when showery weather conditions prevailed in the Saipan area (fig. 2 and table 1), the mixing ratio in the stirred layer was above average and the cloud base below average. This was the time when the lowest inversion was observed between the large clouds, where large areas entirely free of clouds were present. However, the inversion will not always be lower than the lowest cloud bases under such conditions. Local ceilings in showers may be considerably lower (as on May 4). On the other hand, when the inversion was relatively high, many small cumulus clouds were observed, instead of a few large ones. To summarize, the inversion height and cloud height will vary in the same sense for the following reasons:

(1) The lower the inversion, the higher the mixing ratio in the stirred layer and the lower the condensation level.

(2) The lower the condensation level, the lower must the dry downward currents extend to compensate for the moist upward currents.

(3) The addition of moisture to the stirred layer by showers, lowering the cloud base, occurs under conditions favoring powerful local subsidence between clouds, lowering the inversion.

Moisture Discontinuity. The strength of the moisture discontinuity at H_1 is determined by three variables:

(1) The mixing ratio of the stirred layer ($\overline{w}_{st}$). This quantity varied through a total range of 2.4 g/kg (table 1). A rough estimate of $\overline{w}_{st}$ can be obtained from the cloud height (except in showers) by assuming that it is the 95 percent relative humidity level at a potential temperature of 299.5°K (fig. 4).

(2) The mixing ratio in the layer above the transition zone. The mean mixing ratio in the layer from 2,500 to 4,000 ft ($\overline{w}_{25-40}$ in table 1) is used as a measure of this quantity. The range of variation is 5.4 g/kg, or more than twice the variation in the stirred layer. The average value of $\overline{w}_{25-40} - \overline{w}_{st}$ is 3.9. Only about half the moisture transition takes place in the inversion layer ($\Delta w_1 = 2.0$). It is seen from figure 6 that Δw_1 can be estimated roughly from a knowledge of $\overline{w}_{25-40}$ alone. A correction can be applied for the deviation of $\overline{w}_{st}$ from the mean. The variation of $\overline{w}_{25-40}$ with time is shown in figure 2 for both airplane and radiosonde observations. Excluding measurements made in clouds, the airplane and radiosonde values agree quite well. Values of $\overline{w}_{25-40}$ vary with the degree of convective activity, values of less than 12 being associated with prevailing flat cumulus clouds and values over 14 occurring in showery weather. It is possible then to obtain a preliminary estimate of w_1 without making a detailed sounding. Since the temperature discontinuity is very small, it is seen from the definition of M (see footnote, p. 4) that $\Delta M_1 - 5\Delta h_1$ will depend mainly upon Δw_1. Figure 7 shows $\Delta M_1 - 5\Delta h_1$ plotted against Δw_1. The line $\Delta M_1 - 5\Delta h_1 = -7\Delta w_1 - 1$ can be used to give an approximation to $\Delta M_1 - 5\Delta h_1$.

(3) The depth of the transition layer (Δh_1). In the present series of measurements, the transition layer varied in thickness from 100 to 800 ft, with an average value of 300 ft. This is the most difficult of the factors to take into account, since it seems to have little relation to the other atmospheric characteristics observed. One reason for this apparently erratic variation may be the lack of sufficiently closely spaced readings in the vicinity of the transition zone for accurate determination of its depth. It was pointed out above (sec. 4.2) that 55 percent of the measured values depend only on two readings. However, from the plot of Δh_1 against Δw_1 in figure 8, it is seen that 65 percent of the values of Δh_1 are 100 or 200 ft, roughly equal to the altitude interval between readings, but at values of Δw_1 of 2 g/kg or greater, larger values of Δh_1 appear. Within the accuracy of measurement, $\Delta h_1 = 125\ \Delta w_1$ seems a fair approximation. Although the points are too scattered to warrant any quantitative conclusions, it appears that there is a limiting vertical gradient of moisture in the inversion, the greater decreases of moisture requiring deeper transition layers. This fact would be useful in estimating ΔM_1, the modified index inversion, using an estimated $\Delta M_1 - 5\Delta h_1$ obtained as indicated in (2) above. In fact, for $\Delta w_1 < 2$,

for practical purposes (within the limits of our measurements) Δh_1 is constant; ΔM_1 can be estimated directly from Δw_1, as shown in figure 9. More accurate measurements will be required before a definite relation can be found between Δh_1 and other variables. For instance, it is likely that Δh_1 will vary considerably with different convective patterns. The partial stirring that occurs in a layer of fractocumulus clouds may act to spread out the discontinuity, while the sinking currents between towering cumulus or cumulonimbus clouds may tend to concentrate the transition in a narrow zone. It would follow then that Δw_1 is determined mainly by large-scale subsidence and convergence associated with varying synoptic situations, while Δh_1 is a function of local subsidence associated with individual convective cells. Figure 10 shows an example of a sounding with a very moist stirred layer, low cloud base and small Δw_1, and one with a dry stirred layer, high cloud base and large Δw_1.

5. HIGHER INVERSIONS

5.1 Theory

It is well known that in the trade-wind current, a temperature inversion with a decrease of mixing ratio commonly occurs at some level between about 4,000 and 10,000 ft, the height varying with the synoptic situation. This inversion is known as the "trade inversion" or the "top of the moist layer." It is usually the upper limit of general cumulus development, although individual towering cumulus or cumulonimbus clouds will sometimes penetrate it. During periods of widespread shower activity the stable layer may disappear temporarily. Its height is in the range of theoretical values of the top of the layer of turbulent influence given in table 5.

5.2 Measurements

Seven of the 12 airplane soundings reaching 8,000 ft showed a stable layer based at some altitude between 3,500 and 7,000 ft, the average altitude being 5,000 ft. Of twenty-one 12-hourly radiosonde records for the period from May 6 to May 16, 16 show a relatively stable layer, also appearing at an average altitude (H_2) of 5,000 ft. As shown by the radiosondes, the average vertical extent of the inversion is 1,900 ft, the average temperature lapse is 0.9°C, and the average mixing ratio lapse is 4.6 g/kg (fig. 1 and table 2). Approximate readings taken from plotted soundings for the period April 28 to May 6 show the same pattern, but with somewhat higher values of H_2. This inversion fluctuates with the weather (fig. 2), generally following the general cumulus tops and disappearing in periods of abnormal instability. The airplane soundings and radiosondes do not agree well on either the height or the intensity of the inversion, but this may be due to the fact that the airplane soundings were made at a different time and up to 150 mi distant from the radiosondes. The H_2 inversion showed considerable changes in these distances. The strongest inversion was observed by the airplane 50 mi east of Saipan at 1123 GMT on May 9, and 50 mi farther east no inversion could be found. The Saipan radiosondes showed a stable layer on this occasion, the top agreeing well with that measured by the airplane 50 mi east, but the base appearing considerably lower on the radiosonde. In no case was a moisture discontinuity found of sufficient intensity to form a duct (M-inversion). However, neither the radiosondes nor the airplane soundings in this altitude range were

sufficiently detailed to be conclusive. It is possible that the normal cumulus deck is a result of mechanical stirring, and the H_2 is the limit of frictional influence. This would help explain the otherwise puzzling fact that temperatures measured within cumulus clouds were always lower than those measured in the clear environment. However, the values of H_2 agree with theoretical values of the height of the layer of turbulent influence (based on the 4,000-ft wind at Saipan) only in order of magnitude; their variations show no apparent correlation. Our measurements are insufficient to justify drawing any conclusions on this point.

REFERENCES

Byers, H.R., General Meteorology, McGraw-Hill Book Co., New York, 1944, 645 pp.

CINCPAC-CINCPOA Bulletin No. 4-45, "Climatology and Oceanography of Operational Areas of the Western Pacific," U.S. Pacific Fleet and Pacific Ocean Areas, 1945.

Montgomery, R.B., "Modified Index Distribution Close to the Ocean Surface," Radiation Laboratory Report 651, Massachusetts Institute of Technology, Cambridge, Massachusetts, 1944.

Petterssen, S., Weather Analysis and Forecasting, 1st ed., McGraw-Hill Book Co., New York, 1940, 503 pp.

Sverdrup, H.U., Oceanography for Meteorologists, Prentice-Hall, New York, 1942, 246 pp.

U.S. Weather Bureau, Atlas of Climatic Charts of the Oceans, prepared under the supervision of Willard F. McDonald, W.B. Pub. No. 1247, Washington, D.C., U.S. Government Printing Office, 1938, 65 pp.

Table 1.--Summary of airplane observations

Date	Local time	Location	θ_{st}	T_s	w_s	$\overline{w}_{st}$	ΔM_s	H_{cl}	H_1	Δh_1	ΔT_1	Δw_1	ΔM_1	v_{20}	ΔT_{20-40}	$\overline{w}_{25-40}$	Weather (general)	Weather (soundings)
Apr.																		
29	1046*	Just NE Saipan	298.7	26.9	22.0	16.0	45	17	18	1	0	2.5	-10	03	-2.5	12.0	Few cum.	Through layer of scatt. cum.
29	1132	100 mi NE	298.9	27.1	22.2	16.2	46	--	14	1	+0.5	1.6	- 8	03	-4.6	13.7	Clear.	Clear.
29	1249	100 mi NE	298.7	27.1	22.2	16.2	46	--	16	2	0	0.7	+ 3	02	Too few readings		Clear.	Clear.
30	1518	Farallon I.	299.7	27.9	23.3	15.7	53	22	16	2	0	0.5	+ 5	05	-4.2	12.9	Towering cum. to 1,000 ft.	Clear.
May																		
3	1413	90 mi N	299.4	27.6	22.9	16.6	45	19	14	2	-0.2	1.0	+ 2	10	-3.6	12.9	2/10 cum., cum. nimb. 80 mi S.	Clear.
3	1506	Farallon I.	299.4	27.6	22.9	17.2	42	17	16	3	0	2.9	- 6	10	-3.5	13.4	2/10 cum., line of cum. nimb. 80 mi S.	Clear.
4	1402	100 mi N	299.6	27.8	23.1	18.1	36	9	12	3	-0.3	1.9	+ 1	17	-3.6	15.0	Many scatt. show., broken cum., few cum. nimb.	Clear.
4	1501	100 mi N	299.6	27.8	23.1	17.9	37	16	16	2	-0.1	1.2	+ 1	17	-3.3	14.5	6/10 cum. tops 7,500 ft, line of cum nimb. S.	Clear.
6	1416	100 mi N	298.9	27.1	22.2	17.5	32	11	15	2	+0.1	2.9	-10	16	-3.3	13.3	10/10 altostrat., 2/10 small cum.	Clear.
6	1511	100 mi N	299.0	27.2	22.4	17.3	37	11	14	2	+0.3	1.1	- 4	16	-2.8	12.7	10/10 altostrat., 2/10 small cum.	Clear.
7	1348	20 mi NE	299.8	28.0	23.5	17.2	45	21	22	1	+0.1	0.7	- 1	12	-3.8	14.0	Scatt. cum. to 5,000 ft, few to 7,000 ft.	Clear.
7	1348*								--	-	----	---	---		-5.1	14.9		In cum. clouds, light rain in top.
7	1520	20 mi NE	Not enough readings											12	-5.0	14.1	Scatt. cum.	Clear.
8	1345	40 mi NE	299.5	27.7	23.0	17.0	43	21	18	2	+0.2	1.2	0	12	-2.4	13.4	3/10 cum. to 4,000 ft, few tops to 10,000 ft.	Clear.
8	1345*								--	-	----	---	-		-4.2	14.5		In or under clouds.
8	1520	Near Saipan	299.5	27.7	23.0	16.3	47	21	20	not enough readings		1.9	--	12	-2.9	12.0	Scatt. cum.	Clear.
9	1123	50 mi E	299.2	27.4	22.6	17.3	40	18	15	1	+0.2	0.7	- 1	08	-4.1	13.4	Few cum.	Clear.
9	1254	100 mi E	299.5	27.7	23.0	16.4	47	--	15	1	+0.2	2.1	-10	08	-3.0	10.9	Few cum.	Clear.
9	1415	150 mi E	299.6	27.8	23.1	16.0	50	--	13	5	-0.5	2.6	+ 4	08	-3.9	12.0	Few patches altostrat., no low cloud.	Clear.

Table 1.--Summary of airplane observations (continued)

Date	Local time	Location	θ_{st}	T_s	w_s	$\bar{w}_{st}$	ΔM_s	H_{cl}	H_1	Δh_1	ΔT_1	Δw_1	ΔM_1	v_{20}	v_{20-40}	$\bar{w}_{24-40}$	Weather (general)	Weather (soundings)
May																		
9	1500	150-20 mi E	299.6	27.8	23.1	16.2	49	17	17	1	0	3.6	-20	08	-3.1	9.6	Few patches altostrat., few cum.	Clear.
12	1445*	35 mi E	299.6	27.8	23.1	17.6	40	17	26*	2	+0.3	2.4	- 2	16	-2.3	11.6	4/10 cum. tops to 2,500 ft.	Through area of scatt. cum.
12	1550	20 mi E	299.6	27.8	23.1	16.2	49	17	16	5	+0.1	5.3	-11	16	-3.7	10.8	4/10 cum.	Clear area.
13	1324	25 mi E	299.7	27.9	23.3	16.3	49	--	19	6	-0.6	3.5	-11	12	-2.6	11.7	Scatt. cum.	Clear.
13	1402	25-65 mi E	299.6	27.8	23.1	16.2	49	19	18	5	-0.2	4.4	- 8	12	-2.6	11.4	Scatt. cum.	Clear.
13	1430	70 mi E	299.6	27.8	23.1	16.8	45	20	18	8	-1.0	4.8	- 2	12	-2.7	11.2	Scatt. cum.	Clear.
13	1500	70-10 mi E	299.6	27.8	23.1	16.5	47	20	23† 16	1 1	0 -0.2	1.9 0.9	- 7 - 1	12	-3.0	11.3	Scatt. cum. tops to 2,800 ft., few to 9,000 ft.	Clear.
14	1352	20 mi E	299.6	27.8	23.1	17.5	41	13	18 11	2 1	+0.1 0	1.9 0.4	- 4 + 1	19	-3.9	13.9	3/10 cum. to 11,000 ft, cum. nimb. S.	Clear spot
14	1439	40 mi E	299.4	27.6	22.9	17.9	36	15	17 10	2 5	-0.3 -0.8	0.5 2.1	+ 4 + 6	19	-3.8	14.8	2/10 cum to 9,000 ft in being, cum. nimb. E.	Clear area.
14	1520	70 mi E	---- Points too scattered ----					15	15 11	1 1	0 0	0.8 0.7	- 4 - 1	19	-4.1	14.5	5/10 cum. to 8,000 ft.	Clear.
16	1334	50 mi E	299.8	28.0	23.5	16.7	48	20	23	2	+0.2	3.0	- 6	12	-2.6	12.8	3/10 small cum., few tops to 5,000 ft.	Clear spot.
16	1406	50 mi E	299.8	28.0	23.5	16.7	48	22	22	3	-0.6	2.7	+ 7	12	-3.1	13.3	3/10 small cum., few tops to 5,000 ft.	Clear.
16	1406*								--	-	----	---	---		-5.0	14.5		In or under clouds.
16	1437	50 mi E	299.8	28.0	23.5	16.5	49	22	25	1	+0.1	1.3	- 4	12	-2.4	13.2	3/10 small sum., few tops to 5,000 ft.	Clear.
Average			299.5	27.7	23.0	16.8	44	17.5	17.1	2.4	-0.1	2.0	- 3	--	-3.5	12.9		
Maximum			299.8	28.0	23.5	18.1	53	22	26	8	+0.5	5.3	+ 7	--	-5.1	15.0		
Minimum			298.7	26.9	22.0	15.7	32	9	10	1	-1.0	0.4	-20	--	-2.3	9.6		

* Observation through clouds.

† Where there appeared to be two transition layers, both heights H_1 and corresponding Δh_1, ΔT_1, Δw, and ΔM_1 are given, separated by a bar (-).

Table 2.--Summary of radiosonde observations

Date	Local time	H_2 (ft)	Δh_2 (ft)	ΔT_2 (°C)	Δw_2 (g/kg)	ΔT_{20-40} (°C)	w_{25-40} (g/kg)	dt/dh_{100} (°C/1,000 ft)	T_{100} (°C)	w_{100} (g/kg)	v_{40} (mi/h)
April 28	2300	4,800	1,200								06
" 29	1100	4,600	1,700								07
" 29	2300	4,400	3,400								03
" 30	1100	7,500	2,500								04
" 30	2300	9,400	700								02
May 1	1100	7,600	2,000								05
" 1	2300	7,500	2,100								05
" 2	1100	--	--	Approximate values							07
" 2	2300	5,900	3,700								08
" 3	1100	--	--								10
" 3	2300	5,700	700								12
" 4	1100	8,200	1,700								16
" 4	2300	4,900	1,300								21
" 5	1100	5,600	600								16
" 5	2300	--	--								12
" 6	1100	--	--								19
" 6	2300	5,900	1,000	+0.9	-3.8	-2.1	19.3	-2.4	14.3	7.6	19
" 7	1100	5,400	1,000	+0.3	-2.2	-1.7	9.9	-2.4	11.1	4.0	15
" 7	2300	6,000	5,000	+3.0	-5.4	-2.9	12.5	-0.7	11.7	9.7	14
" 8	1100	5,800	800	+0.9	+0.6	-3.7	12.8	-2.2	10.4	4.2	13

Table 2.--Summary of radiosonde observations (continued)

Date	Local time	H_2 (ft)	Δh_2 (ft)	ΔT_2 (°C)	Δw_2 (g/kg)	ΔT_{20-40} (°C)	w_{25-40} (g/kg)	dt/dh_{100} (°C/1,000 ft)	T_{100} (°C)	w_{100} (g/kg)	v_{40} (mi/h)
May 8	2300	5,000	1,000	0	-0.8	-4.2	11.2	-1.6	8.7	4.0	11
" 9	1100	5,000	3,500	-3.2	-10.1	-2.8	12.3	-2.1	12.5	--	12
" 9	2300	--	--	--	--	-3.7	13.6	-1.8	8.1	4.3	04
" 10	1100	--	--	--	--	-3.4	15.2	-1.7	14.4	7.0	18
" 10	2300	--	--	--	--	-4.5	15.0	-2.0	8.1	7.3	18
" 11	1100	4,500	700	-0.5	-1.0	-3.6	11.0	-1.7	12.9	7.5	26
" 11	2300	4,600	800	+0.7	-3.7	-2.0	19.1	-3.1	14.1	5.7	18
" 12	1100	4,500	2,300	+1.5	-6.6	-4.2	11.1	-2.3	13.2	2.1	16
" 12	2300	5,000	1,700	-0.4	-7.0	-4.3	13.8	-2.1	10.2	2.2	14
" 13	1100	4,500	800	0	-1.2	-3.4	12.1	-1.6	10.5	--	08
" 13	2300	4,000	600	0	-1.0	-2.4	11.0	-1.8	10.0	2.6	18
" 14	1100	4,700	--	--	--	-3.9	14.9	-1.6	10.2	8.6	24
" 14	2300	--	--	--	--	-5.0	11.4	-1.8	6.1	6.8	16
" 15	1100	4,600	2,800	-2.6	-6.5	-4.9	16.8	-2.3	11.1	8.2	15
" 15	2300	5,500	3,000	-3.3	-8.8	-3.6	14.3	-2.1	10.5	4.0	16
" 16	1100	--	--	--	--	-3.5	12.7	-1.1	14.1	3.7	17
" 16	2300	5,100	3,200	-3.9	-7.5	-3.4	13.4	-1.9	8.7	2.1	14
Average		5,000	1,900	-0.9	-4.6	-3.5	13.5	-2.0	11.1	5.4	13
Maximum		6,000	5,000	+1.5	+0.6	-5.0	19.3	-3.1	14.4	9.7	26
Minimum		4,000	600	-3.9	-10.1	-1.7	9.9	-0.7	6.1	2.1	02

Table 3.--Surface parameters e_s, w_s, M_s as functions of T_s

T_s (°C)	e_s (mb)	w_s (g/kg)	M_s*
26.4	33.8	21.4	410
26.6	34.2	21.6	412
26.8	34.6	21.8	413
27.0	35.0	22.1	415
27.2	35.4	22.4	416
27.4	35.8	22.6	417
27.6	36.2	22.9	418
27.8	36.6	23.1	419
28.0	37.1	23.5	421
28.2	37.6	23.8	423
28.4	37.9	24.0	424
28.6	38.4	24.3	426
28.8	38.8	24.6	427
29.0	39.4	24.9	428
29.2	39.9	25.2	430
29.4	40.4	25.6	432
29.6	40.8	25.8	434
29.8	41.3	26.1	435
30.0	41.7	26.4	437

* $M_s = \frac{79}{T_s} (1{,}013 + 4{,}800 \frac{e_s}{T_s})$

Table 4.--ΔM_s as a function of Δw_s

Δw_s	ΔM_s
4.0	28
4.2	30
4.4	31
4.6	33
4.8	34
5.0	35
5.2	37
5.4	39
5.6	41
5.8	42
6.0	43
6.2	45
6.4	46
6.6	47
6.8	48
7.0	50
7.2	51
7.4	52
7.6	54
7.8	55
8.0	57

Table 5.--Height of the layer of frictional influence (in feet, lat. 15°N)

	b	0.5		1.0		2.0		5.0		10.0	
v	a	100	3,300	100	3,300	100	3,300	100	3,300	100	3,300
5		1,800	1,400	2,000	1,500	2,100	1,600				
10		3,600	2,900	4,000	3,000	4,300	3,200	4,800	3,500		
15		5,400	4,300	6,000	4,500	6,400	4,800	7,300	5,300		
20				8,000	6,000	8,600	6,400	9,700	7,000	11,000	7,200
25					7,500	11,000	8,000	12,000	8,800	14,000	9,000

a = height of wind measurement, feet.

b = height of ocean waves, feet.

v = wind velocity, miles per hour.

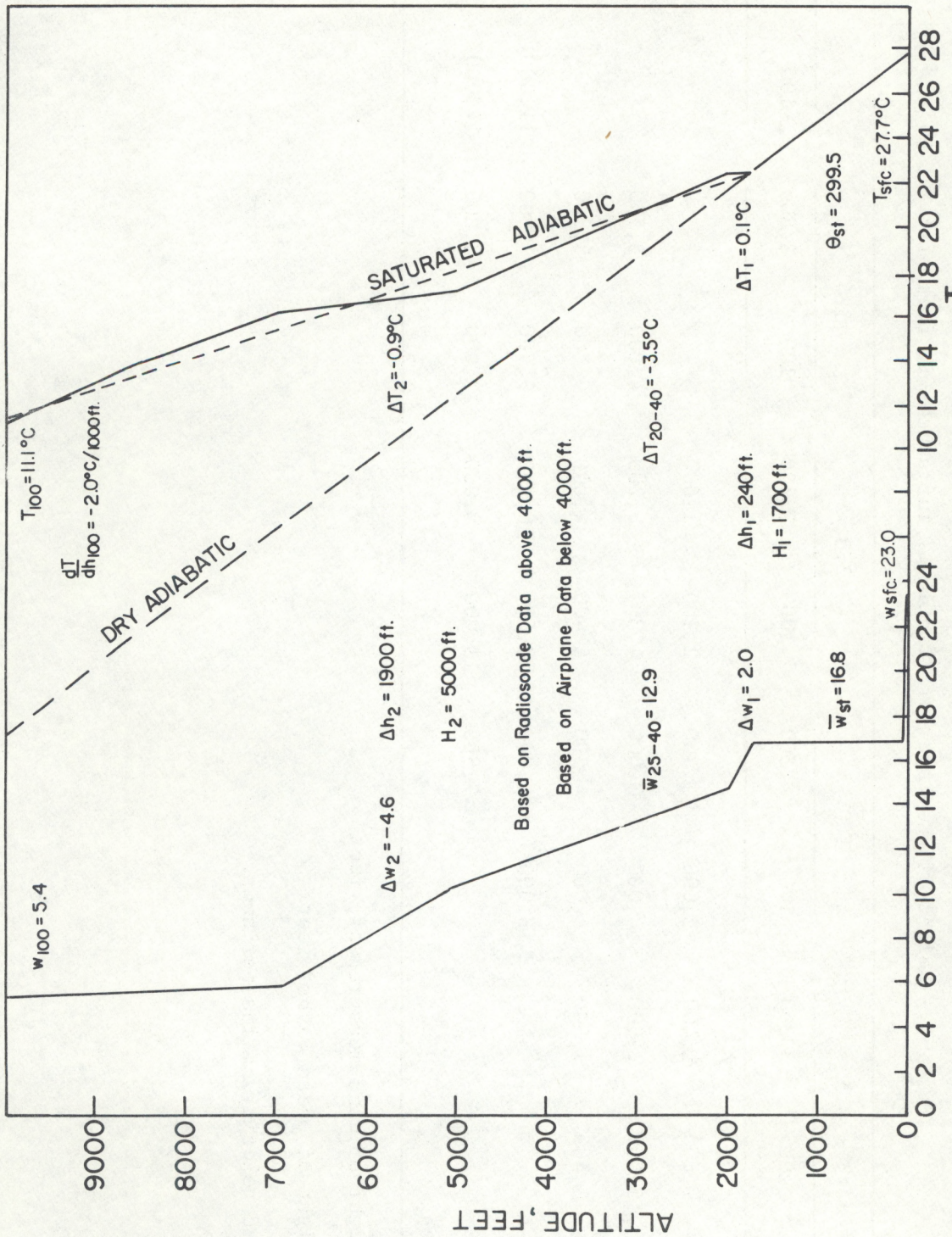

Figure 1.--Average characteristics of the lower atmosphere.

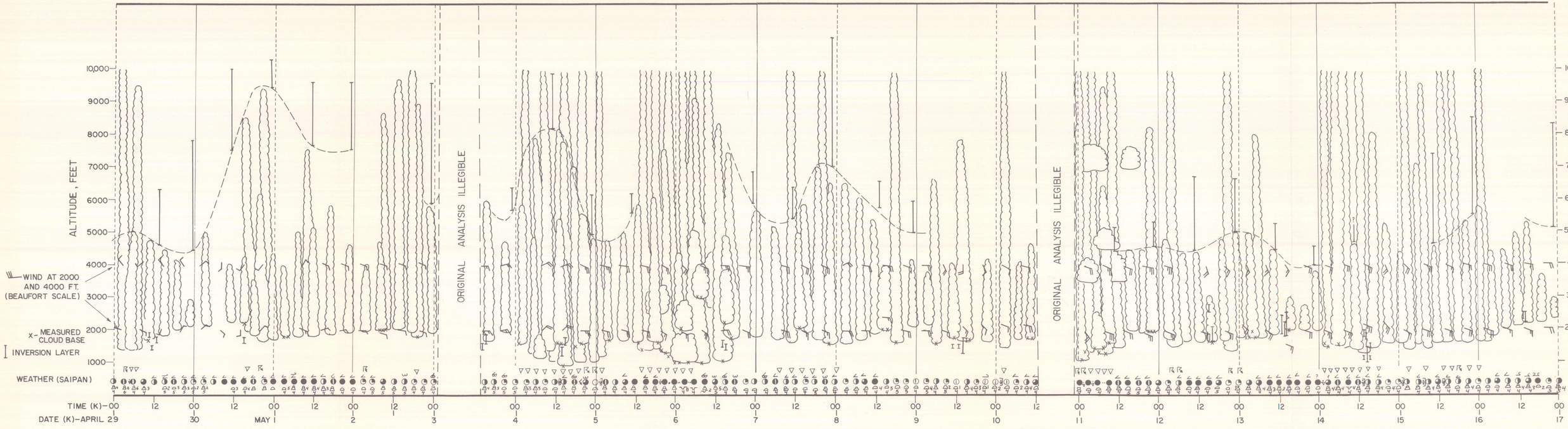

Figure 2.--Time cross section.

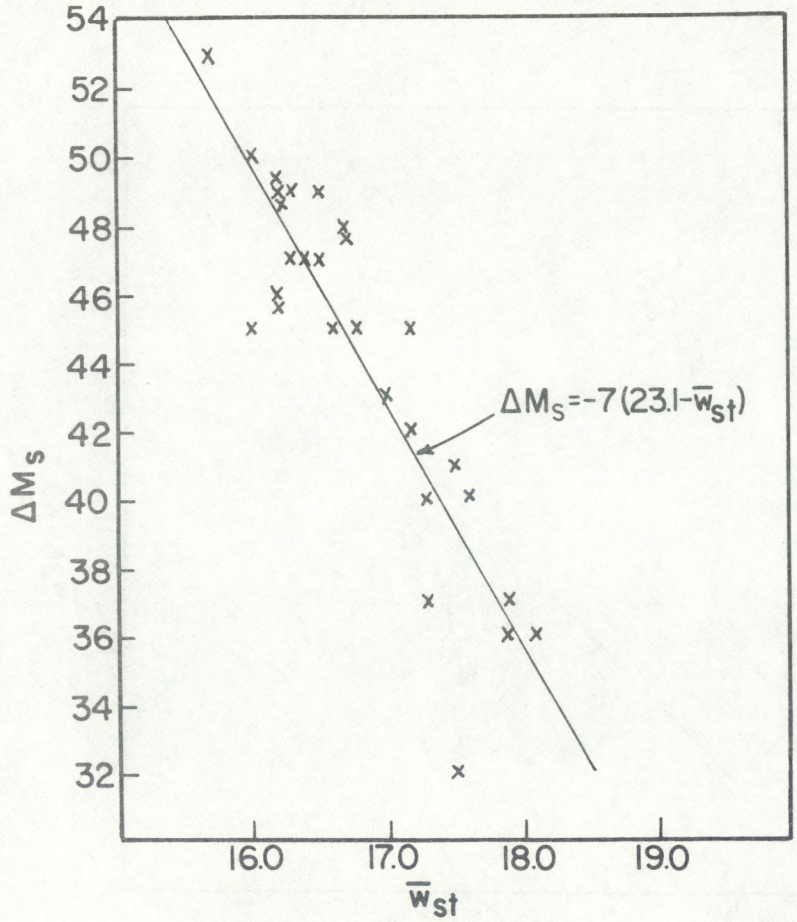

Figure 3.--ΔM_s vs. $\bar{w}_{st}$.

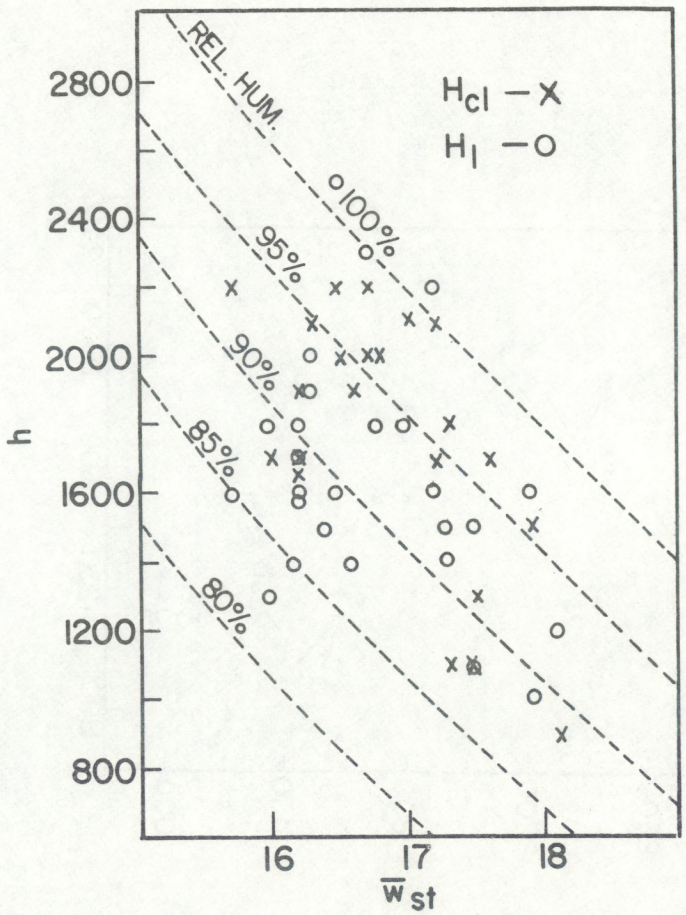

Figure 4.--H_l and H_{cl} vs. $\bar{w}_{st}$.

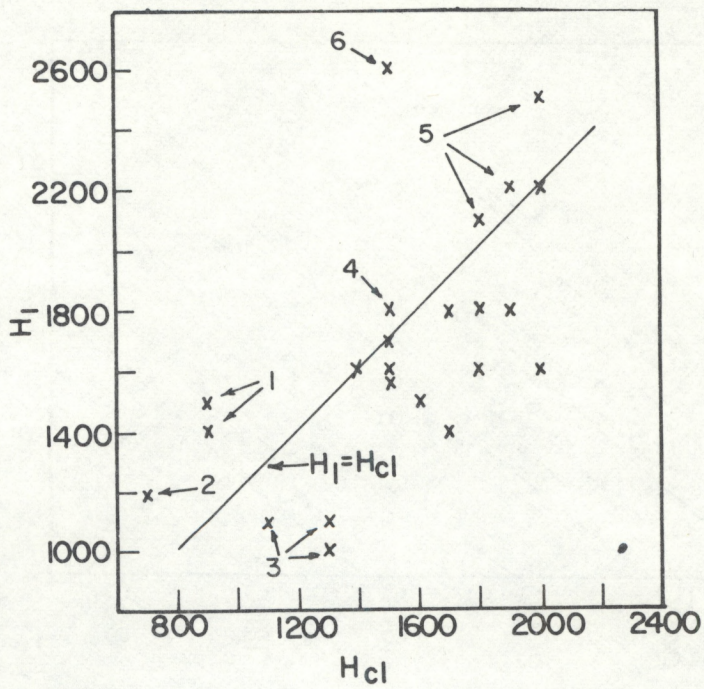

Figure 5.--H_1 vs. H_{cl}. 1 - 2/10 small cumulus; 2 - shower; 3 - towering cumulus and cumulonimbus; 4 - through scatter cumulus area; 5 - 3/10 small cumulus; 6 - top of scattered cumulus.

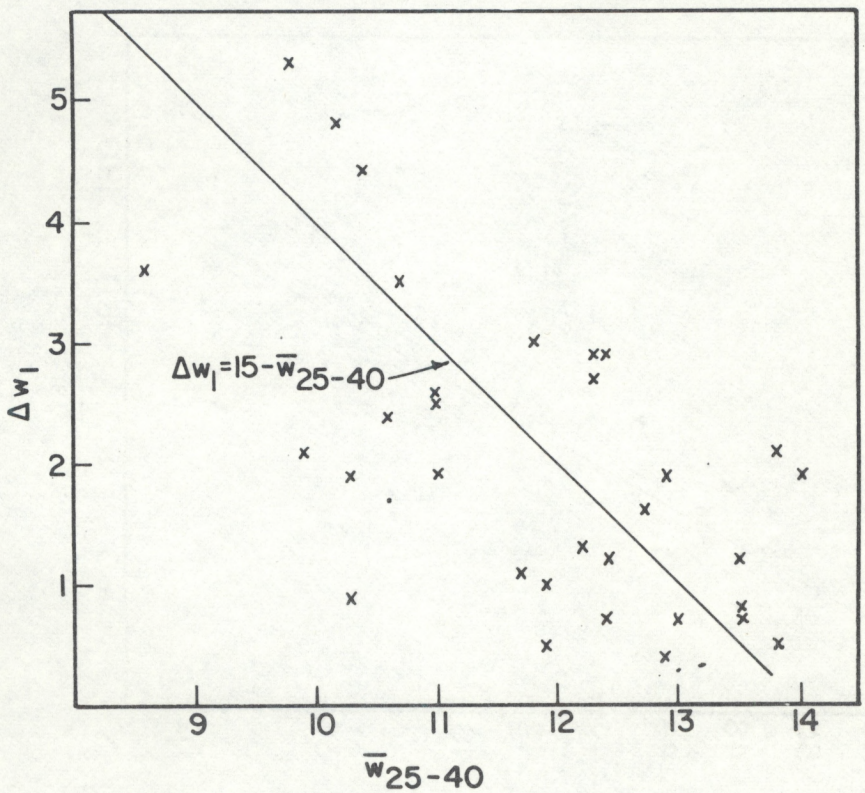

Figure 6.--Δw_1 vs. $\overline{w}_{25-40}$.

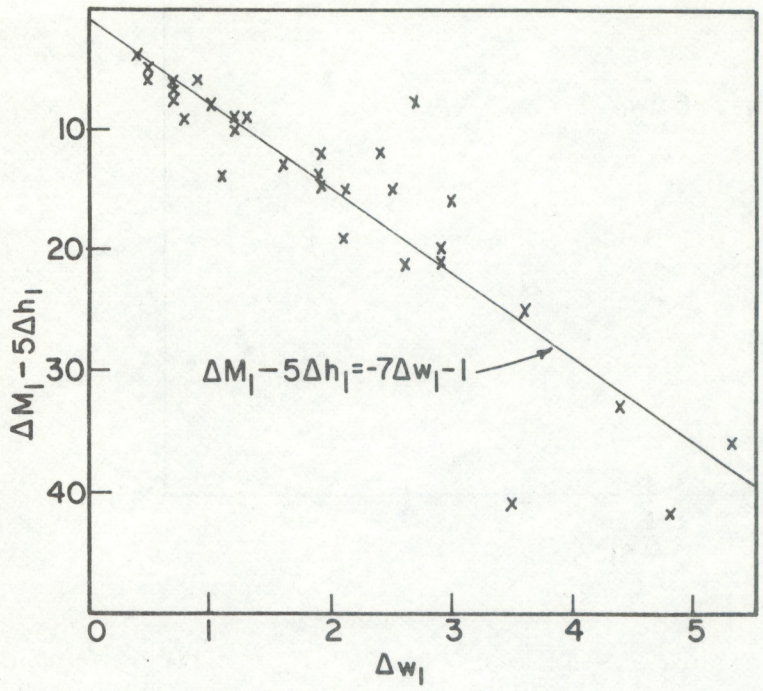

Figure 7.--ΔM_1-$5\Delta h_1$ vs. Δw_1.

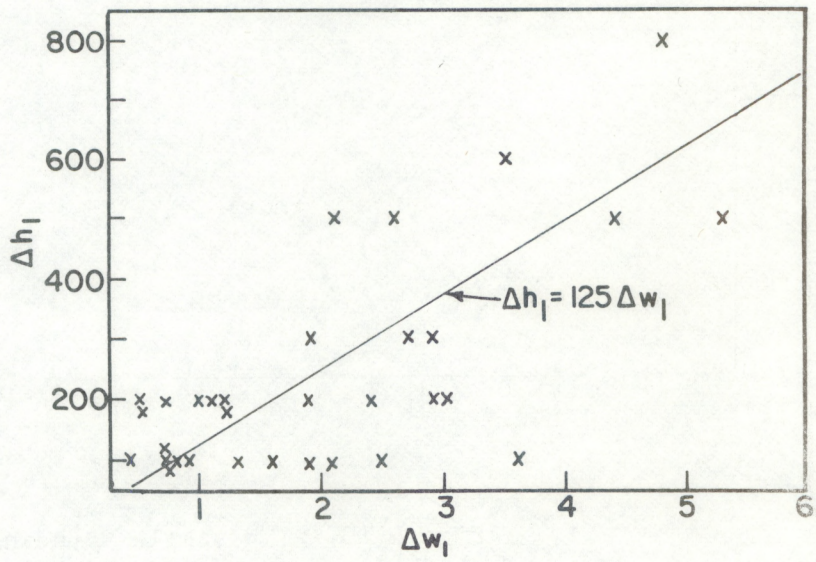

Figure 8.--Δh_1 vs. Δw_1.

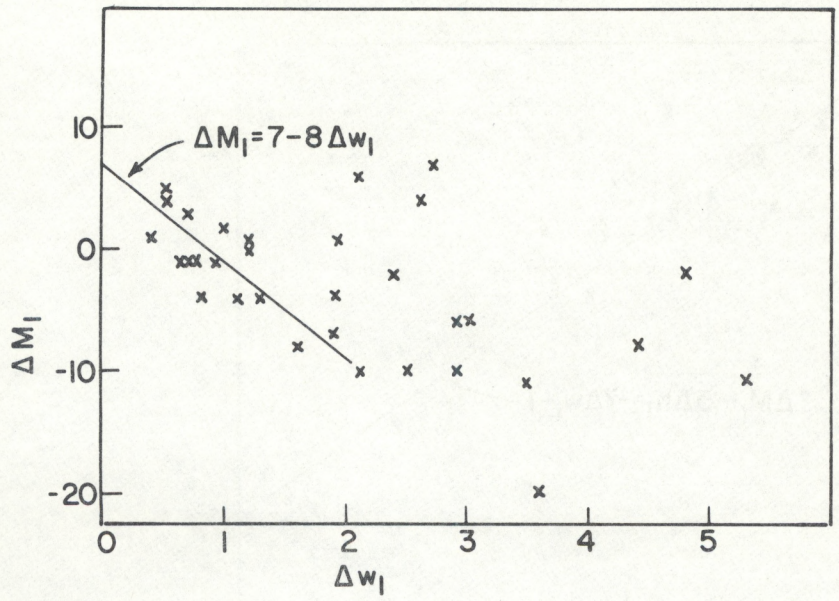

Figure 9.--ΔM_1 vs. Δw_1.

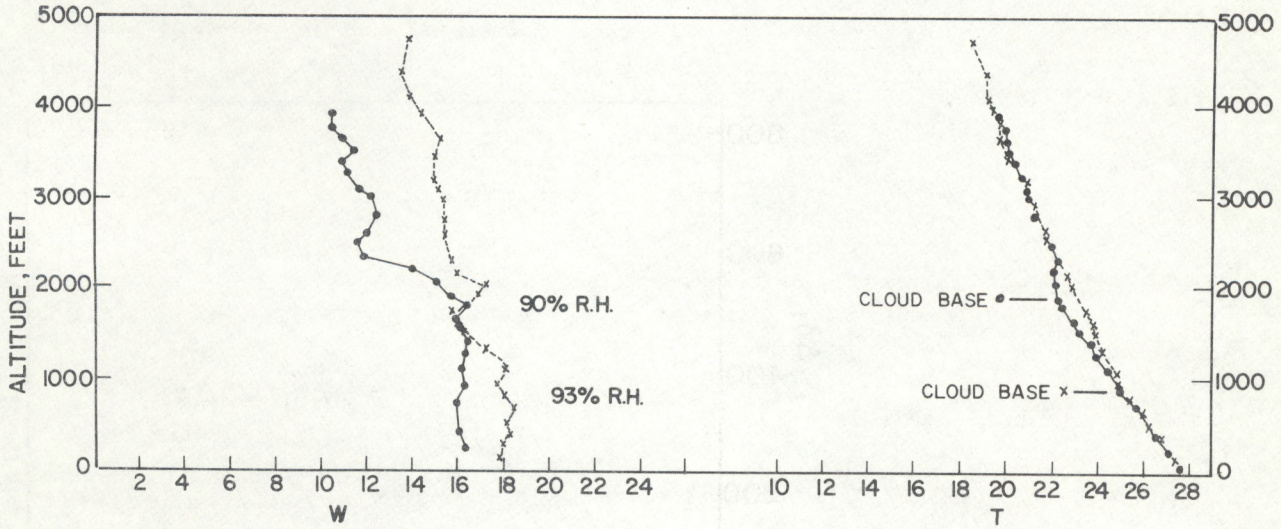

Figure 10.--Two sample soundings.